Available online at www.sciencedirect.com
SCIENCE DIRECT®
ELSEVIER
International Journal of Solids and Structures 42 (2005) 4722–4737
INTERNATIONAL JOURNAL OF SOLIDS and STRUCTURES
www.elsevier.com/locate/ijsolstr

Green's function-based multiscale modeling of defects in a semi-infinite silicon substrate ☆

B. Yang [a,*], V.K. Tewary [b]

[a] Department of Mechanical and Aerospace Engineering, Florida Institute of Technology, Melbourne, FL 32901, USA
[b] Materials Reliability Division, National Institute of Standards and Technology, Boulder, CO 80305, USA

Received 20 July 2004; received in revised form 25 January 2005
Available online 3 March 2005

Abstract

We have developed a Green's function (GF) based multiscale modeling of defects in a semi-infinite silicon substrate. The problem—including lattice defects and substrate surface, i.e., an extended defect, at different length scales—is first formulated within the theory of lattice statics. It is then reduced and solved by using a scale-bridging technique based on the Dyson's equation that relates a defect GF to a reference GF and on the asymptotic relationship of the reference lattice-statics GF (LSGF) to the continuum GF (CGF) of the semi-infinite substrate. The reference LSGF is obtained approximately by solving the boundary-value problem of a super-cell of lattice subject to a unit point force and under a boundary condition given by the reference CGF. The Tersoff potential of silicon, germanium and their compounds is used to derive the lattice-level force system and force constants and further to derive the continuum-level elastic constants (of the bulk silicon, needed in the reference CGF). We have applied the method to solve for the lattice distortion of a single vacancy and a single germanium substitution. We have further calculated the relaxation energy in these cases and used it to examine the interaction of the point defects with the (traction-free) substrate surface and the interaction of a single vacancy with a relatively large germanium cluster in the presence of the substrate surface. In the first case, the point defects are found to be attracted to the substrate surface. In the second case, the single vacancy is attracted to the germanium cluster as well as to the substrate surface.

1. Introduction

Multiscale modeling is required in the engineering of most, if not all, nanodevices due to the involvement of physical phenomena at multiple length (and time) scales and to the limited computer power against a

☆ Publication of the National Institute of Standards and Technology, an agency of the US Government; not subject to copyright.
* Corresponding author. Tel.: +1 321 674 7713; fax: +1 321 674 8813.
E-mail address: boyang@fit.edu (B. Yang).

0020-7683/$ - see front matter © 2005 Elsevier Ltd. All rights reserved.
doi:10.1016/j.ijsolstr.2005.01.019

huge number of degrees of freedom (DOFs) if the system is resolved entirely at the atomistic level. The quasicontinuum method and other combined atomistic and continuum methods employing a handshaking technique at the atomistic and continuum interface may be employed to carry out the task of eliminating redundant DOFs of a nanosystem (Kohlhoff et al., 1991; Tadmor et al., 1996; Shenoy et al., 1999; Arroyo and Belytschko, 2002, among others). These methods are based on a finite-element (FE) setting, where regions of anticipated low-gradient deformation are approximated as continuum and others are left in the discrete atomistic form. These FE-type methods essentially adopt an adaptive mesh with those atomistic regions being discretized at the finest size that is "physically admissible"—atomic spacing. The interatomic potential is used as the constitutive law, in place of the continuum elasticity, plasticity, viscoplasticity, etc., to describe the behavior of constituents. Such FE-type methods hold great advantage in that the implementation is straightforward. They can handle virtually any geometry and any material system that the classical FE method can do. Their disadvantage is that many characteristics of a system that can be useful to reduce the computational effort are wasted, for example, in the case of micro/nanodevices of electronics and optoelectronics developed on the base of a semiconductor layered structure (Harrison, 2002). The literature has suggested that the layered base structure can be analytically treated before the entire device structure with defect-like features is handled and that this can significantly reduce the total computational effort (Yang and Pan, 2003). On the contrary, the (three-dimensional, heterogeneous) thin-layer structure can be extremely difficult for a FE-type method to deal with.

Recently, Tewary (2004) has proposed an alternative multiscale modeling of mechanical behavior of nanostructures using continuum and lattice-statics Green's functions (GFs), which has shown promising accuracy and efficiency (see also, Tewary and Yang, 2003). A GF is the solution to a system consisting of geometry, material and loading condition. The loading condition may be a point force, a point heat source, or a point charge, in addition to a homogeneous boundary condition. The GF describes the propagation of information from a point source over the domain. It can be viewed as a characteristic behavior of the whole system. When it is applied to solving various related problems, those features of specified material, geometry and boundary condition are carried over. In the other words, when solving a problem with changes upon the system where the GF is derived, the only numerical effort is virtually to handle those changes—this sometimes is convenient and efficient for parametric studies. The field of GFs has been advanced in three separate routes, namely, on the quantum mechanical, lattice and continuum levels (see, e.g. Kittel, 1987; Tewary, 1973; Ting, 1996)—here we consider only the last two levels. A continuum GF (CGF) assumes that the material can be treated as a continuum so that the concepts of stress and strain and theories based on them can be applied. A lattice GF, on the contrary, does not make this assumption, and naturally treat the material as a discrete system. (The lattice GF includes lattice-statics GF (LSGF) and lattice-dynamics GF. Only the LSGF is considered here.) Because a LSGF accounts for more detail of a material, it is a closer approach to the reality than a CGF. However, for the same reason, it takes much longer time and many more computer resources to calculate a LSGF compared to a CGF. Therefore, a strategy of integrating these two approaches in a balance of physical approximation and computational efficiency would greatly advance the modeling of nanosystems involving physical process at and between the lattice and continuum scales.

The multiscale GF (MSGF) method originally proposed by Tewary (2004) can deal with general defects that alter both the force system and force constants in a lattice. This method is based on the Dyson's equation that relates the defect and perfect (generally speaking, reference) LSGFs and on the asymptotic relationship of the perfect infinite-space LSGF and CGF. It has been applied to model the vacancy, a point defect, at the atomistic level and the substrate free surface, an extended defect, at the macroscopic level in copper (Tewary, 2004). It has also been applied to model the germanium quantum dot (QD) in a semi-infinite silicon substrate (Tewary and Yang, 2003). However, since the perfect infinite-space LSGF was derived by the Fourier transform and the complementary part of free surface by using the continuum theory, this formulation is limited to the case where the lattice defect is remote to the substrate surface.

Prior to that work, there had been efforts in solving the core structure of dislocations by imposing flexible GF boundary conditions (Sinclair et al., 1978; Rao et al., 1998). In the work, the perfect infinite-space/plane LSGF and CGF were used and an iterative procedure of relaxation of the boundary condition was adopted to obtain the nonlinear behavior at the core of dislocations. Since the perfect LSGF was used instead of the defect LSGF, the change of force constants was not accounted for. This corresponds to the classical continuum approach of defects as inclusions ignoring the elastic mismatch, whilst the Tewary formulation corresponds to the continuum approach of defects as inhomogeneous inclusions taking into account both the elastic mismatch and eigenstrain between the defects and matrix (Eshelby, 1956; Mura, 1987).

In the present work, we reformulate the MSGF method for the modeling of defects in nanostructures (Tewary, 2004; Tewary and Yang, 2003). We introduce a more flexible and efficient way of evaluating the MSGF, and demonstrate it in a semi-infinite crystalline silicon substrate. The present technique can model point defects very close to the substrate surface. More importantly, it holds the potential for extension to more complicated cases, for instance, a multilayered nanostructure with defects and defect-like features such as QDs of strong technological interest (Harrison, 2002); the work on a multilayered nanostructure is in progress and will be discussed elsewhere. Unlike in the previous work, in solving the Dyson's equation, we take the reference GF to be either the CGF or the LSGF of the semi-infinite reference lattice, depending on the distance of the source and field points. The LSGF of the semi-infinite reference lattice is approximately obtained by solving the boundary-value problem of a super-cell of lattice subject to a unit point force and under a CGF boundary condition. In the special case where the super-cell reaches the substrate surface, the force-free—traction-free—boundary condition is imposed along that side. Thus, the obtained LSGF is a hybrid LSGF rather than the "true" LSGF, which is virtually unavailable. The validity of the imposition of a CGF boundary condition around a lattice cell relies on the asymptotic approach of the discrete medium to its continuum counterpart as the distance of the source and field points increases. It also relies on the appropriate approach of a lattice-level source by a continuum one. In the present work, the first condition is satisfied (except right along the substrate surface) since the matrix is a homogeneous medium and since only the statics—at the long-wave length limit (Kunin, 1982)—is considered. The second condition is also satisfied since our transition of the lattice to the continuum is made within the reference system where the source is a force; there is no difference between forces at the lattice and continuum levels although there may be a difference in their responses at the different scales. However, if the source is a point defect, such as a vacancy, substitution or interstitial, its continuum approach is, rigorously speaking, untenable. For example, a plausible approach of a single vacancy may be a spherical cavity with force dipoles (Townsend, 1976). It requires the parameters of cavity size and dipole magnitude. While the latter parameter can be evaluated from the interatomic potential, the cavity size cannot be defined well, not to mention the rough assumption of a spherical shape, because the lattice distortion around the vacancy can be significant in response to the local force dipoles and/or to a remote loading. Here, we put forth a scheme of multiscale modeling of defects that makes no approximation on the defects beyond the lattice-statics level. It first rigorously bridges the lattice- and continuum-level behaviors of a force in the reference system based on their asymptotic relationship. It then applies the reference GFs to solve the Dyson's equation for the defect GF and further for the lattice distortion of the defect system. Numerical error (other than the round-off error), if any, should occur in the approximation of the reference LSGF by a CGF. It can be easily evaluated and controlled in the relatively simple reference system without a defect. Furthermore, this needs to be done only once for all defect systems based on the same matrix. This is obviously advantageous for extensive parametric studies in the design of related nanosystems.

The present paper is organized as follows. In Section 2, we describe the MSGF modeling of defects within the theory of lattice statics. In Section 3, we examine in detail the hybrid LSGF in the specific case of semi-infinite silicon substrate. In Section 4, we apply the MSGF method to solve for the lattice distortion and further for the relaxation energy of a single vacancy, a single germanium substitution and a germanium

cluster in a semi-infinite silicon substrate. The results are used to show the effect of the substrate surface on the lattice distortion and to examine the interaction between the point defects, the relatively large defect of a germanium cluster, and the substrate free surface. The fine features of the lattice distortion near the point defects, which are lost in a continuum modeling of silicon assuming the cubic anisotropy, are revealed in the present solution. In Section 5, conclusions are drawn.

2. Green's function method of defects

We consider a semi-infinite silicon substrate with a free surface. There may be multiple defects such as vacancies and germanium substitutions in the substrate. The system is modeled as a lattice structure, as schematically shown in Fig. 1(a). The lattice knots are numbered by $(i,j,k;l)$, where i,j and k indicate the location of a unit cell, and l indicates the location of a knot within the unit cell and takes value from 1 to 8. Let $(0,0,0;1)$ be on the surface and $k \geqslant 0$. Also, a Cartesian reference is attached, with the origin located at the lattice site $(0,0,0;1)$, and with the axes (x_1,x_2,x_3) directed respectively along the lattice axes (i,j,k). The lattice is diamond-like, made of two sets of face-centered cubic lattice with one shifted by $(1/4,1/4,1/4)$ unit-cell length relative to the other. The $(0\,0\,1)$-axis is normal to the substrate surface. In the bulk state, each lattice knot has four nearest neighbors and twelve second nearest neighbors.

Suppose that the potential V of the defect system is given as a function of atomic position $x_i^{(a)}$. Within the theory of lattice statics, the equilibrium of the defect system requires

$$\frac{\mathrm{d}V}{\mathrm{d}x_i^{(a)}} = 0, \tag{1}$$

where the subscript i indicates the ith (Cartesian) coordinate, and the superscript a indicates the ath atom. The potential may be expanded in a Taylor series around a ground state 0,

$$V = V_0 + \left(\frac{\partial V}{\partial x_i^{(a)}}\right)_0 u_i^{(a)} + \frac{1}{2}\left(\frac{\partial^2 V}{\partial x_i^{(a)}\partial x_j^{(b)}}\right)_0 u_i^{(a)}u_j^{(b)} + \mathrm{o}\left(u_i^{(a)}u_j^{(b)}u_k^{(c)}\right), \tag{2}$$

where $u_i^{(a)}$ indicates the ith displacement component of the a-atom, and the repeated subscript/superscript implies the conventional summation over its range. Approximating the potential up to the quadratic term and substituting it in Eq. (1) yield

$$\phi_{ij}^{(ab)}u_j^{(b)} = f_i^{(a)}, \tag{3}$$

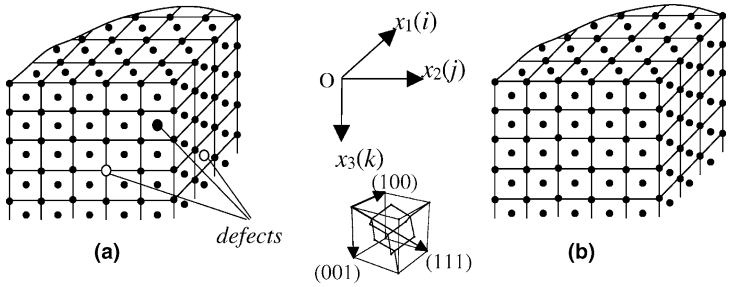

Fig. 1. Schematic drawing of a semi-infinite silicon lattice: (a) with defects (target system); (b) without defects (reference system). The Cartesian coordinates $x_1(i)$, $x_2(j)$, and $x_3(k)$ are established as shown. Also shown is a unit cell of the diamond-like lattice.

where the force and force constants (stiffness matrix) are defined as

$$f_i^{(a)} \equiv -\frac{\partial V}{\partial x_i^{(a)}} \quad \text{and} \quad \phi_{ij}^{(ab)} \equiv \frac{\partial^2 V}{\partial x_i^{(a)} \partial x_j^{(b)}}. \tag{4}$$

A solution to the atomic displacement field $\boldsymbol{u}$ of the defect system can be obtained by inverting the stiffness matrix $\boldsymbol{\phi}$ as

$$u_j^{(b)} = [\phi_{ij}^{(ab)}]^{-1} f_i^{(a)}. \tag{5}$$

Defining $L_{ji}^{(ba)} \equiv [\phi_{ij}^{(ab)}]^{-1}$, the above equation is rewritten as

$$u_j^{(b)} = L_{ji}^{(ba)} f_i^{(a)}. \tag{6}$$

$L_{ji}^{(ba)}$ may be read as, instead of the inverted stiffness matrix, the ith displacement component of the a-atom caused by a unit force applied along the jth direction on the b-atom, namely, the LSGF of the defect lattice system (Tewary, 1973).

Eqs. (5) and (6) imply two different ways of solving the lattice-statics problem. In Eq. (5), the whole stiffness matrix is inverted, i.e., the displacement field of the entire system is solved in a single task. The task can become practically infeasible if the system is large, and can be unnecessary if only a small portion of the total displacement field is of interest. With Eq. (6), if the LSGF, $L_{ji}^{(ba)}$ is available, one can calculate the displacement at individual atoms of interest without involving the entire system. It requires only the values of $L_{ji}^{(ba)}$ between the atoms whose displacements are acquired and atoms where the forces $f_i^{(a)}$ are exerted. The method based on Eq. (6) is called the (classical) LSGF method (Tewary, 1973). However, it is in general not an easy task to find $L_{ji}^{(ba)}$ of an arbitrary defect lattice system.

To find $L_{ji}^{(ba)}$, the stiffness matrix $\boldsymbol{\phi}$ of the defect system in Fig. 1(a) is partitioned as

$$\phi_{ij}^{(ab)} = \phi_{ij}^{0(ab)} + \Delta\phi_{ij}^{(ab)}, \tag{7}$$

where $\boldsymbol{\phi}^0$ is the stiffness matrix of the system excluding the defects, namely, a reference system, as schematically shown in Fig. 1(b), and $\Delta\boldsymbol{\phi}$ is the difference of stiffness matrix between the reference and defect systems. Inverting the matrices in Eq. (7) and rearranging yield

$$L_{ji}^{(ba)} = L_{ji}^{0(ba)} - L_{jk}^{(bc)} \Delta\phi_{kl}^{(cd)} L_{li}^{0(da)}, \tag{8}$$

where $L_{ji}^{0(ba)}$ $(\equiv [\phi_{ij}^{0(ab)}]^{-1})$ is the reference LSGF. Eq. (8) is called the Dyson's equation, relating the LSGF of two different systems, namely, defect and reference systems, through their differential stiffness matrix $\Delta\phi_{kl}^{(cd)}$. Given $L_{ji}^{0(ba)}$, Eq. (8) can be used to solve for $L_{ji}^{(ba)}$. To do so, the solution of $L_{ji}^{(ba)}$ is first sought for all a- and b-atoms within the defect space defined by nontrivial $\Delta\boldsymbol{\phi}$. Then, $L_{ji}^{(ba)}$ is obtained for an arbitrary pair of a- and b-atoms. Finally, the displacement at selected lattice sites is evaluated by using Eq. (6). Therefore, the solution to the defect system is now reduced to find the reference LSGF, $L_{ji}^{0(ba)}$.

The reference LSGF, $L_{ji}^{0(ba)}$ of the semi-infinite lattice may be divided in two parts: the infinite-space part, and the complementary part due to the presence of surface. The infinite-space part may be evaluated by solving the boundary-value problem of a crystallite subject to a unit point force and under a fixed or periodic boundary condition. However, the size of the crystallite can become prohibitively large due to the limited computer power in case that $L_{ji}^{0(ba)}$ is needed between atoms in a wide range of distance, depending on the spatial distribution of nontrivial $\Delta\phi_{kl}^{(cd)}$ and force $f_i^{(a)}$. Alternatively, the infinite-space part may be evaluated by applying the Fourier transformation, where the frequency domain must be truncated in order for a finite number of operations. The truncation of frequency domain is equivalent to the imposition of a fixed boundary condition around a finite-sized crystallite. Tewary (2004) and Tewary and Yang (2003) used the Fourier transformation method to obtain the infinite-space part and used the continuum approach to

calculate the complementary part due to the substrate surface. The drawback of these approaches is the possible prohibitively large size of the working crystallite and the limitation of the location of source from being close to the substrate surface. In the present work, we propose to develop a hybrid reference LSGF by solving the boundary-value problem of a crystallite (i.e., a super-cell of lattice) subject to a unit point force and under a semi-infinite CGF boundary condition. The hybrid LSGF is expected to approach the "true" LSGF as the size of super-cell increases. Then, we apply the hybrid reference LSGF and the corresponding CGF in place of the "true" reference LSGF, $L_{ji}^{0(ba)}$ to solve the Dyson's equation for the defect GF and subsequently for the displacement field of defects, depending on the distance of source and field points. If it turns out that the required super-cell size is fairly small for a reasonable accuracy, the difficulties that occur in the previous approaches can be resolved—this will be verified in the next section. In the present approach, the effect of the discrete lattice around the source, the effect of the substrate surface, and the long- and/or short-range interaction between multiple lattice defects are seamlessly bridged across the different length scales. Furthermore, there is no approximation made upon the lattice defects in the defect system beyond the lattice-statics level. Therefore, it presents a significant advancement in accurate and efficient solution of such multiscale problem of lattice and extended defects.

3. Hybrid lattice-statics Green's function of semi-infinite silicon substrate

Suppose that the reference system of a semi-infinite silicon lattice in Fig. 1(a) is subjected to a unit point force along one of the axes, for instance, the Ith direction, at a specified lattice site A. Assume that there be a unique response of the lattice to the force, namely, the LSGF, under a (homogeneous) boundary condition and a remote radiation condition. The system may also be modeled as a continuum subjected to a unit point force and under corresponding boundary and radiation conditions. The solution is the CGF. The lattice and continuum media modeling the same material are linked by the asymptotic approach of the force constants of the former to the elastic constants of the latter (Maradudin et al., 1971):

$$\phi_{ij}^{(ab)} \to C_{ijkl}(\boldsymbol{x}). \tag{9}$$

The force constants, a second-rank tensor, characterize the interaction between adjacent atoms. The elastic constants, a forth-rank tensor, characterize the local behavior of an infinitesimally small volume element of the material (the local elasticity is assumed). We hypothesize that the LSGF approaches to the CGF as the distance of field point to force increases. Under the condition, given the CGF, the LSGF can be evaluated, as follows.

The equilibrium of the semi-infinite lattice requires Eq. (3) to hold, in which the superscripts a and b take value over the entire system. Let us draw a super-cell of lattice around the unit force, as schematically shown in Fig. 2(a). Layers of atoms that directly interact with any atoms out of the super-cell are identified as boundary atoms, drawn in the light color in the figure. As hypothesized earlier, if their distance to the source, i.e., a point force, is sufficiently large, the displacement of the boundary atoms and all the atoms outside of the super cell can be assigned with the half-space CGF which is available (Pan and Yuan, 2000). By doing so, the equilibrium equation (3) reduces to the following form:

$$\phi_{ij}^{(ab)} u_j^{(b)} = \delta_{Ii}^{(Aa)} \tag{10}$$

with $a \in$ super cell minus boundary atoms, and $b \in$ super cell, where $\delta_{Ii}^{(Aa)}$ is the Dirac delta, which is equal to one if $a = A$ and $i = I$, and equal to zero otherwise. After substituting the CGF for the displacement of the boundary atoms, one can solve Eq. (10) for the displacement at the interior atoms. The solution offers the hybrid LSGF, $H_{Ii}^{0(Aa)}$.

In the special case that the super cell reaches the substrate free surface, the top side of the super-cell is exempted from the identification of boundary atoms, as schematically shown in Fig. 2(b). The atoms on the

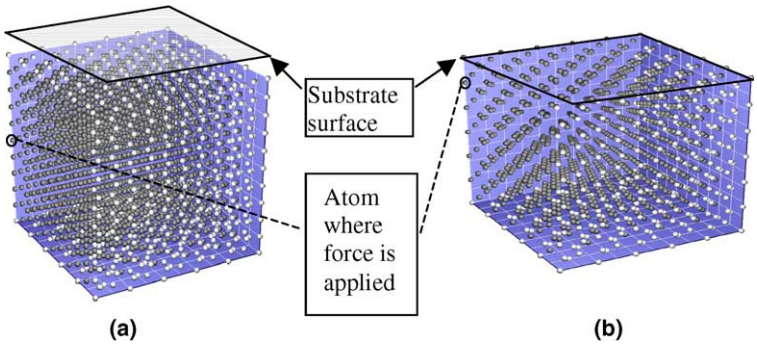

Fig. 2. A super-cell inside a semi-infinite silicon substrate (a quarter is shown): (a) entirely embedded in the substrate; (b) opened at the substrate surface. The interior atoms are shown in dark color and the boundary atoms in light color.

free surface are treated as interior atoms whose displacements are unknown. The CGF boundary condition is imposed upon the boundary atoms at the other five sides of the super-cell as above. Applying Eq. (10), one can solve for the atomic displacement in the super-cell. In this case, the part of the substrate surface close to the force is taken into account on the discrete level, while the rest is treated as a continuum.

The Tersoff potential of carbon, silicon and germanium and their mixtures (Tersoff, 1989) is employed to calculate the force constants of the reference silicon lattice (and of the defect system with vacancies and germanium substitutions to be examined later). The force constants are used further to calculate the elastic constants of the bulk silicon. The Tersoff potential takes into account the interaction of an atom with its first and second nearest neighbors. We programmed the Tersoff potential with the parameters given in his article. The force constants (and forces needed in later simulations) are calculated in a finite-difference scheme by perturbing the position of involved atoms by 0.1% of the (equilibrium) unit-cell size. It is found that the calculated force constants satisfy the following required condition (within the computational accuracy):

$$\sum_{b,j} \phi_{ij}^{(ab)} = 0. \tag{11}$$

It means that a rigid-body translation of the system causes no additional forces.

The semi-infinite lattice described above may be set up by removing the other half from the perfect infinite lattice of silicon in equilibrium. It results that the atoms at least second-nearest-neighbor away from the surface are subjected to no force but the atoms at the surface to some force (as so happens with the Tersoff potential). The net force may either deform uniformly the entire semi-infinite lattice in the vertical direction or cause the atoms at the surface to reconstruct electronically. While the first one is trivial, the second case is likely to happen (Norenberg and Briggs, 1999). In the present work, neither case is considered. Therefore, the defects are limited to a location at least one-unit-cell-spacing away from the surface. To take into account the surface reconstruction, the lattice at the surface should be modified accordingly to experimental observations or to a more advanced simulation. The modification should eliminate any net force in the base system before introducing a defect.

The above force constants of the bulk silicon are used to calculate the corresponding elastic constants. Consider a cube of lattice of, for example, $20 \times 20 \times 20$ unit cells. A boundary condition of displacement, corresponding to a continuum field of straining—one nonzero (strain) component at a time—equal to 0.1%, is imposed upon the two outer layers of atoms. The two layers of atoms are needed as the "boundary" of the cube due to the fact that the Tersoff potential allows for the second-nearest-neighbor interaction. (The same two-layer boundary applies to the super cell in the above GF problem (Fig. 2).) The cube of lattice is

set in equilibrium. Upon that, an interior sub-cube of $10 \times 10 \times 10$ unit cells is taken around the center. The forces exerted on the boundary atoms of the sub-cube by the surrounding atoms are calculated, and are averaged over the surface areas to obtain the "stress" components due to the straining. The process is repeated for all six strain components and all 6×6 elements of the elastic stiffness matrix C_{ij} can be obtained. As expected, the bulk silicon exhibits the cubic anisotropy, holding three independent nontrivial elastic constants: $C_{11} = 0.9044$, $C_{12} = 0.5462$, and $C_{44} = 0.3989$ eV/(Å)^3.

With the Tersoff potential and derived elastic constants, we have examined the hybrid LSGF with the unit point force applied at various depths from the free surface and with various super-cell sizes. The

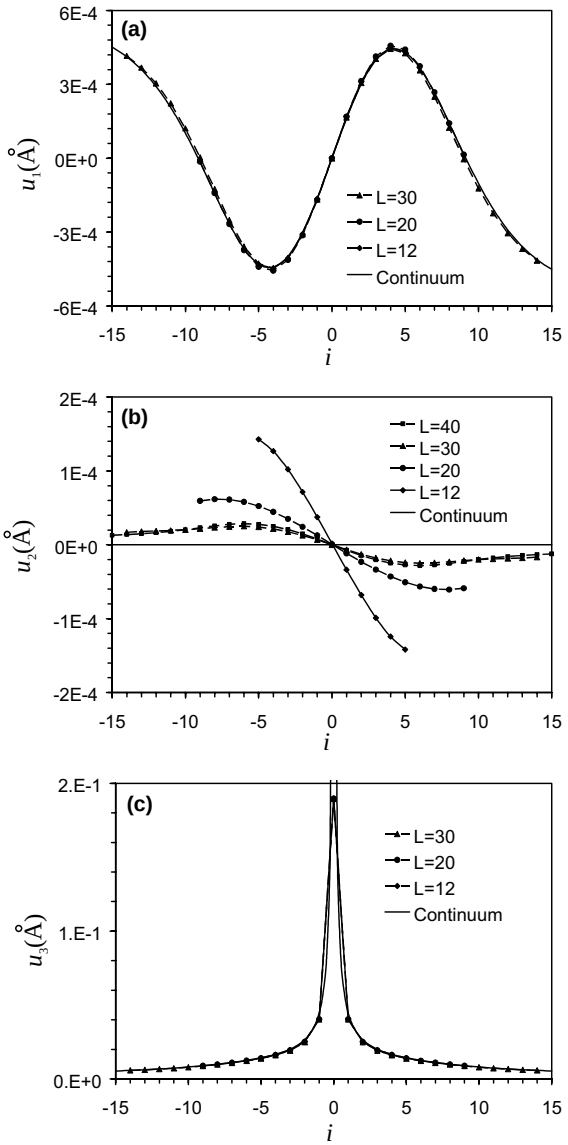

Fig. 3. Variation of displacement components of the point-force GFs along a horizontal line ($i, j = 0, k_f = 5; l = 1$): (a) u_1; (b) u_2; (c) u_3. The force is applied along the x_3-axis and located at the center of the evaluation line ($i = 0, j = 0, k_f = 5; l = 1$).

CGF is evaluated by using the scheme developed by Pan and Yuan (2000). The force is located at ($i = 0, j = 0, k = k_f; l = 1$), and is directed along the x_3-axis, for example. The induced field along a horizontal line passing the force, ($i, j = 0, k = k_f; l = 1$), is evaluated, and the results are shown in Figs. 3 and 4, respectively, for $k_f = 5$ and 1. The sizes—number of unit cells, L—of the super-cell used to calculate the hybrid LSGF are indicated in the figures. In the case that the super-cell reaches the free surface (Fig. 2(b)), the vertical dimension of the super-cell is reduced to be $L/2$ plus the depth of the unit force from the free surface while the horizontal dimensions are both the same as regular, L (Fig. 2(a)). The responses to a unit point force applied along the x_1- and x_2-axes are similar to what are shown in Figs. 3 and 4.

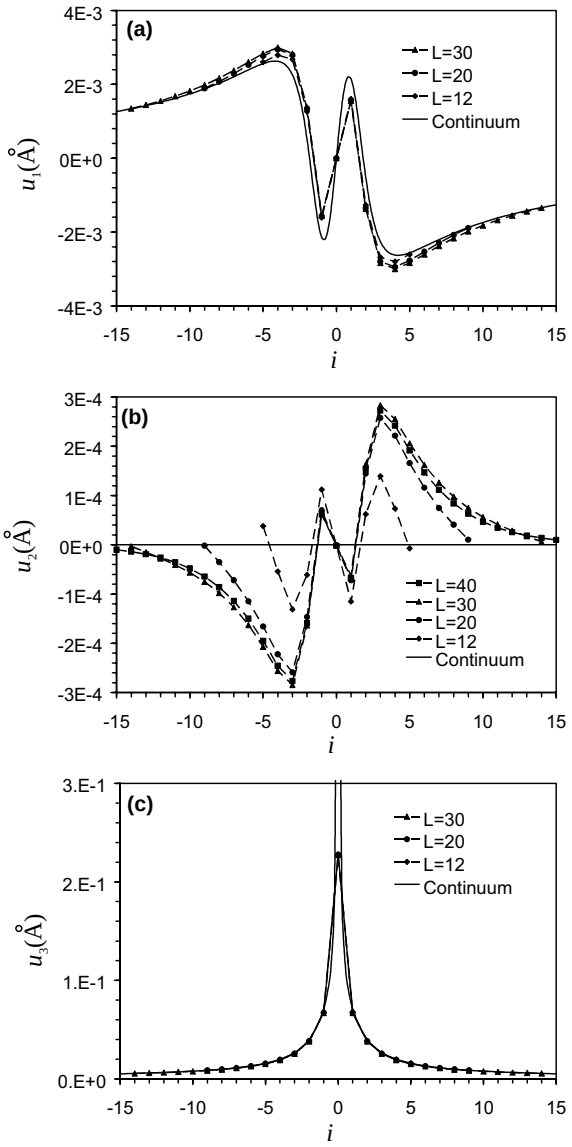

Fig. 4. Variation of displacement components of the point-force GFs along a horizontal line ($i, j = 0, k_f = 1; l = 1$): (a) u_1; (b) u_2; (c) u_3. The force is applied along the x_3-axis and located at the center of the evaluation line, ($i = 0, j = 0, k_f = 1; l = 1$).

In the case with $k_f = 5$, Fig. 3(a) and (c) show that the u_1- and u_3-components of the hybrid LSGF calculated with various super-cell sizes match very well with one another and with the continuum solution. The only exception is the u_3-component in the very vicinity around the unit force where the continuum solution is singular but the lattice solution is finite. However, the difference manifests itself only within a very short distance—one unit-cell spacing—from the force. On the contrary, Fig. 3(b) shows that the u_2-component of the hybrid LSGF calculated with various super-cell sizes shows significant difference from each other and from the continuum solution which is exactly equal to zero. This figure includes the solution with $L = 40$ additional to the ones shown in Fig. 3(a) and (c). The hybrid LSGF with $L = 40$ shows little change from that with $L = 30$. Thus, the hybrid LSGF has converged with super-cell size, or say, the "true" LSGF (of all three components) has been obtained, around $L = 30$. Since the LSGF takes into account the lattice-level asymmetry of the medium about the coordinate planes, its u_2-component is nontrivial along the evaluation line, while the CGF solution assuming the cubic anisotropy is equal to zero along the same line. This effect fades away as the field point gets away from the force. The remote behavior eventually approaches the prediction of the continuum theory. Therefore, all the three displacement components show an asymptotic approach from the lattice to the continuum behavior as the distance from the source increases.

In the case with $k_f = 1$, the unit force is located very close to the free surface. Compared to the previous case, Fig. 4(a) and (b) show a strong effect of the free surface on the u_1- and u_2-components of the GFs. The profiles of these two components are characteristically different from those shown in Fig. 3(a) and (b). The effect of the discrete lattice on the u_1-component is more pronounced than in the previous case. The u_1-component is offset from the CGF solution in a quite large distance from the force. Apart from these differences, the hybrid LSGF behaves similarly to the previous case with a force located deep inside the substrate.

4. Analysis of defects

In the previous sections, we have described the modeling of defects based on the Dyson's equation, and developed the hybrid LSGF by realizing the asymptotic approach of LSGF to CGF, in a semi-infinite silicon substrate. It has been shown that the hybrid LSGF and the CGF can be used to substitute for the "true" LSGF respectively in a short and a long distance from the force in the half-space substrate. By doing so, the Dyson's equation can be solved efficiently and accurately for the defect GF and subsequently for the lattice distortion of defects in the presence of the substrate surface. Therefore, we have put forth a scheme of multiscale modeling of defects that first rigorously bridges the lattice- and continuum-level behaviors of a point force in the reference system and then seamlessly bridges the lattice- and continuum-level behaviors of defects in the defect system. The numerical error (other than the round-off error), if any, should occur in the calculation of the hybrid LSGF of the reference system, which can be easily estimated and controlled. There is no approximation made upon the defects beyond the lattice-statics level. In the following, we apply the MSGF method to examine the lattice distortion of point defects, including a single vacancy and a single germanium substitution, in the presence of a substrate surface. Furthermore, we examine the interaction energy of the point defects with the substrate surface, and the interaction energy of a single vacancy with a relatively large spherical germanium cluster in the semi-infinite silicon substrate. The Tersoff potential (Tersoff, 1989) is employed to describe both the defect and reference systems.

4.1. Lattice distortion of point defects

First, we examine the lattice distortion due to a single vacancy and a single germanium substitution, in the semi-infinite silicon substrate. Since the Tersoff potential allows for the first- and second-nearest-neighbor interactions, the defect space involves 16 additional atoms around the defect site. The numerical results of the induced atomic displacement around the two point defects are shown respectively in Figs. 5 and 6.

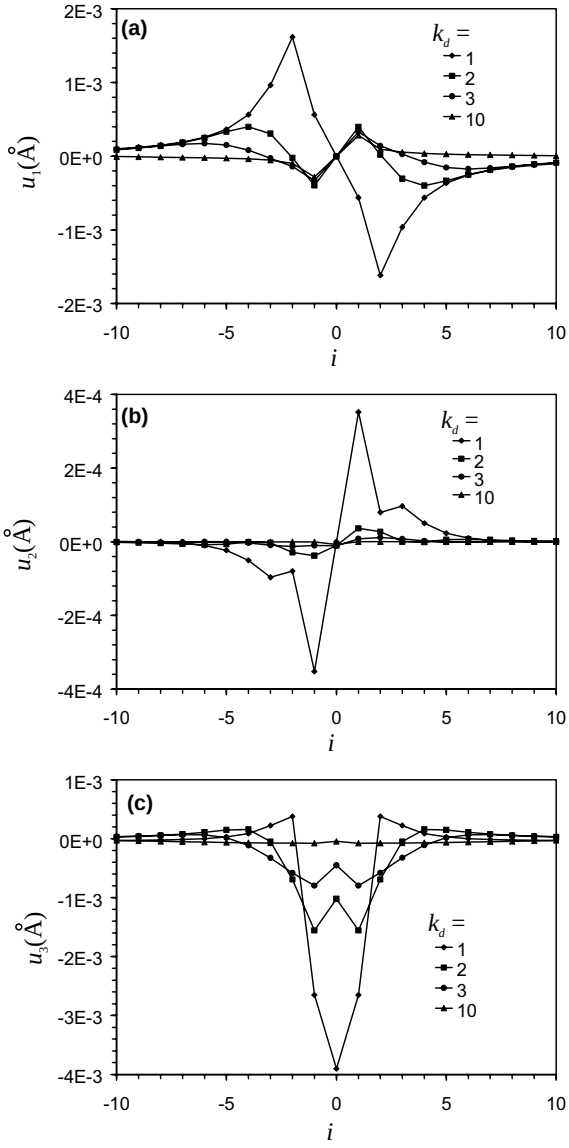

Fig. 5. Variation of atomic displacement components due to a single germanium substitution along a horizontal line ($i,j = 0$, k_d; $l = 1$): (a) u_1; (b) u_2; (c) u_3. The substitution is located at the center of the evaluation line, ($i = 0, j = 0$, k_d; $l = 1$), with various k_d as indicated.

The point defects are located at ($i = 0, j = 0, k = k_d$; $l = 1$), with various depths k_d. The atomic displacement is acquired along a horizontal line passing the defects, ($i, j = 0, k = k_d$; $l = 1$). In Fig. 6, since the atom is missing at the site of vacancy, no displacement is attached to that point.

In both Figs. 5 and 6 of germanium substitution and vacancy, one can see that the effect of the substrate (free) surface is significant on the lattice distortion when the defects are close to the substrate surface. However, the effect fades away quickly as the depth increases. When the defects are deep inside the substrate (with $k_d = 10$), the u_2- and u_3-components are nearly equal to zero, as expected. Only the u_1-component is left to be finite.

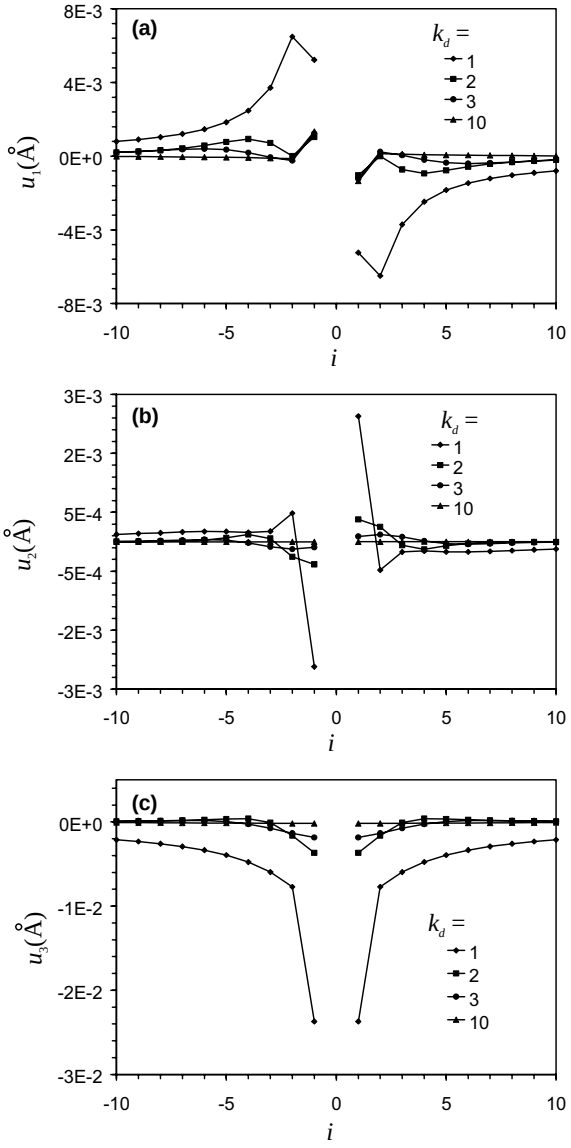

Fig. 6. Variation of atomic displacement components due to a single vacancy along a horizontal line ($i,j = 0$, k_d; $l = 1$): (a) u_1; (b) u_2; (c) u_3. The vacancy is located at the center of the evaluation line, ($i = 0, J = 0$, k_d; $l = 1$), with various k_d as indicated.

In Fig. 5(a) of germanium substitution, the variation of u_1-component indicates that the germanium substitution pulls the surrounding atoms horizontally closer to itself when depth $k_d = 1$, but pushes them away when $k_d = 10$. It implies that the presence of the substitution may exercise opposed effects on the X-ray measurement and alike, depending on its depth from the surface. In Fig. 6(a) of vacancy, it is shown that the defect always pulls horizontally closer to itself the surrounding atoms for any depth k_d of the defect.

In the case of germanium substitution, the u_3-component exhibits a strong oscillation, especially when the depth, k_d is small, compared to the case of vacancy, as shown in Figs. 5(c) and 6(c). The oscillation is spanned in a quite large distance, about a few unit-cell lengths, from the defect. The substrate surface

attracts the atoms very close to the substitution but repels the rest. In the case of vacancy, the substrate surface attracts all the atoms.

The behavior of the u_2-component in both cases of vacancy and germanium substitution revealed in Figs. 5(b) and 6(b) would be lost in the continuum model assuming the cubic anisotropy of matrix and spherical dilatational defects (Eshelby, 1956; Mura, 1987). When the defects are deep inside the substrate ($k_d = 10$), the MSGF solution of this displacement component is nearly equal to zero, consistent with the continuum solution. When the defect gets close to the substrate surface, this displacement component becomes nontrivial due to the effect of the lattice asymmetry manifested by the presence of the substrate surface. In contrast, the continuum model predicts a zero value of this component independent of k_d.

4.2. Interaction between point defects and substrate surface

Upon the solution of atomic displacement field, the relaxation energy of a point defect introduced to the substrate can be calculated. The relaxation energy is defined by

$$E_{\mathrm{re}} \equiv f_j^{(b)} u_j^{(b)} = f_j^{(b)} L_{ji}^{(ba)} f_i^{(a)}. \tag{12}$$

The interaction energy of a point defect with substrate surface is defined by

$$E_{\mathrm{in}} \equiv (E_{\mathrm{re}})_{\mathrm{D+S}} - (E_{\mathrm{re}})_{\mathrm{D}} - (E_{\mathrm{re}})_{\mathrm{S}}, \tag{13}$$

where $(E_{\mathrm{re}})_{\mathrm{D+S}}$ is the relaxation energy of the point defect in the half-space substrate, $(E_{\mathrm{re}})_{\mathrm{D}}$ is the relaxation energy of the point defect located deep inside the substrate, and $(E_{\mathrm{re}})_{\mathrm{S}}$ is the relaxation energy of the surface alone and is conceptually different from the surface energy. Since the surface is free of net force, $(E_{\mathrm{re}})_{\mathrm{S}} = 0$.

We have calculated the interaction energy of a single vacancy and a single germanium substitution with the free surface of the semi-infinite silicon substrate. The point defects are placed at various depths from the substrate surface. They are placed at least one unit-cell length from the surface due to the uncertainty of the surface lattice structure as discussed before. The numerical results are plotted in Figs. 7 and 8 for the vacancy and germanium substitution, respectively. In both cases, the magnitude of interaction energy increases as the depth of defect decreases. The variation becomes abrupt as the defects get close to the surface, between one and two unit-cell lengths. It indicates that the substrate free surface attracts both of the defects. The magnitude of interaction energy of the vacancy (and hence the gradient) is much higher than that of the germanium substitution, by about two orders of magnitude. This does not mean that the

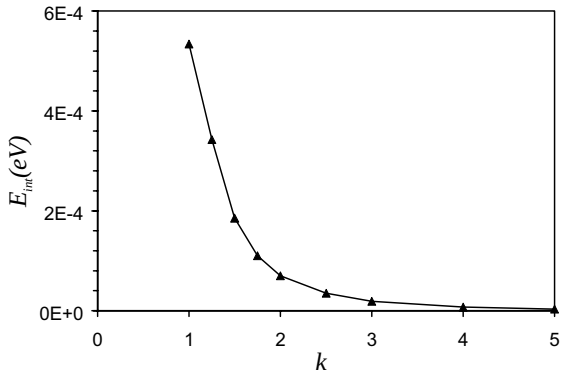

Fig. 7. Variation of interaction energy between a germanium substitution and substrate surface with depth of the substitution from the substrate surface.

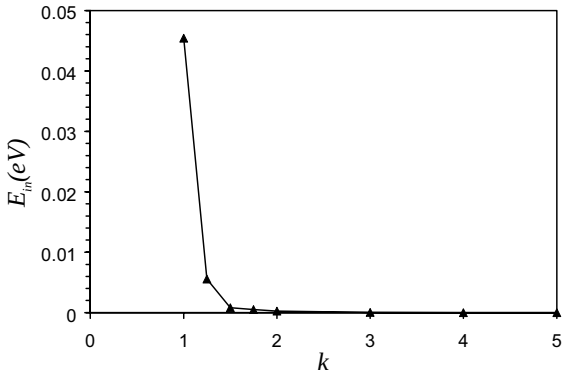

Fig. 8. Variation of interaction energy between a vacancy and substrate surface with depth of the vacancy from the substrate surface.

vacancy should migrate toward the free surface faster than the Germanium substitution since the process is determined also by the energy barrier. The energy barrier could be much higher on the vacancy than on the germanium substitution. The lattice-statics approach can provide the driving force for the migration of a defect. However, the energy barrier must be determined by a more sophisticated approach—the first-principle simulations.

4.3. Interaction of vacancy with germanium cluster and substrate surface

Finally, we examine the interaction of a single vacancy with a spherical germanium cluster (a relatively large substitution particle) in the semi-infinite silicon substrate, as schematically shown in Fig. 9. We define the interaction energy of the vacancy with the germanium cluster and substrate surface by

$$E_{\text{in}} \equiv (E_{\text{re}})_{\text{V+Ge+S}} - (E_{\text{re}})_{\text{Ge+S}} - (E_{\text{re}})_{\text{V}}, \tag{14}$$

where $(E_{\text{re}})_{\text{V+Ge+S}}$ is the relaxation energy of the vacancy and germanium cluster in the half-space substrate, $(E_{\text{re}})_{\text{Ge+S}}$ is the relaxation energy of the germanium cluster in the half-space substrate excluding the vacancy, and $(E_{\text{re}})_{\text{V}}$ is the relaxation energy of the vacancy deep inside the half-space substrate excluding the germanium cluster.

The simulation is carried out with the center of the germanium cluster being fixed at ($i = 0, j = 0, k = 10$; $l = 1$). The germanium cluster consists of 147 atoms occupying five shells of lattice sites around the center.

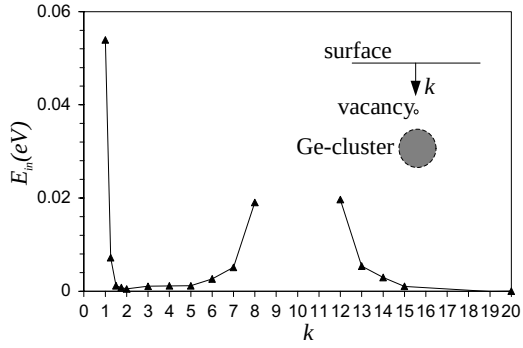

Fig. 9. Variation of interaction energy between a vacancy, germanium cluster and substrate surface with depth of the vacancy from the substrate surface.

A shell consists of lattice sites in the same distance from the center. The first shell consists of the four first-nearest neighbors, the second shell the twelve second-nearest neighbors, and so forth. The diameter of the nominally spherical cluster is about 2 nm. The vacancy is placed at various depths from the substrate surface, but outside of the germanium cluster. Its coordinates are given by $(i = 0, j = 0, k = k_v; l = 1)$. The numerical result is plotted in Fig. 9.

The interaction energy of the vacancy with the germanium cluster and substrate (free) surface increases as the vacancy originally deep inside the substrate moves toward the germanium cluster. It decreases after the vacancy passes and keeps moving away from the germanium cluster toward the substrate surface. Finally it increases abruptly when it gets close to the substrate surface. The variation indicates that the point defect is attracted to the germanium cluster as well as the substrate free surface. The driving force is given by the gradient of the variation, which can be used to further study the migration of the defect in the presence of the various attractors involving multiple length scales.

5. Conclusion

We have developed a novel computational technique to efficiently and accurately solve the multiscale problem of defects in a semi-infinite silicon substrate using LSGF and CGF. It is based on the Dyson's equation that relates a defect GF to a reference CGF and on the asymptotic relationship of the reference LSGF and CGF of the semi-infinite silicon substrate. Since the reference LSGF is unavailable, a hybrid reference LSGF is proposed to replace it, which is obtained by solving the boundary-value problem of a super-cell of lattice subject to a unit point force and under a CGF boundary condition. The validity of the approximation has been demonstrated numerically for the semi-infinite silicon substrate described by the Tersoff potential (Tersoff, 1989). We have substituted the hybrid reference LSGF and reference CGF for the ''true'' LSGF to solve the Dyson's equation for the defect GF of the defect system and subsequently to solve for the atomic displacement field due to the defects. Therefore, we have developed a scheme of multiscale modeling of defects that makes no approximation of the defects beyond the lattice-statics level. The bridging of the lattice- and continuum-scale behaviors is rigorously established in the reference system with a force as the source. The resulting numerical error (other than the round-off error) can be easily estimated and controlled, and this needs to be done only once for all defect systems based on the same matrix. This is advantageous for extensive parametric studies of related nanosystems, relative to the FE-type methods where the error control is done on a case-by-case base.

We have applied the MSGF method to solve for the lattice distortion of point defects, including a single vacancy and a single germanium substitution, in a semi-infinite silicon substrate. It is found that the atomic displacement fields are influenced significantly by the presence of the substrate free surface. Upon the solution of the atomic displacement field, we have calculated the interaction energy of the point defects with the substrate surface. Both of the point defects are attracted to the surface. The driving force increases abruptly when the defects are close to the surface. Finally, we have examined the interaction of a single vacancy with a relatively large germanium cluster in the semi-infinite substrate. The point defect is attracted to the germanium cluster as well as the substrate surface. The present formulation can provide the driving force for the migration of point defects in the matrix within the lattice-statics theory. It requires only the interatomic potential as the experimental input.

References

Arroyo, M., Belytschko, T., 2002. An atomistic-based finite deformation membrane for single layer crystalline films. Journal of the Mechanics and Physics of Solids 50, 1941–1947.

Eshelby, J.D., 1956. The continuum theory of lattice defects. In: Seitz, F., Turnbull, D. (Eds.), Solid State Physics: Advances in Research and Applications. Academic Press Inc., Publishers, New York.

Harrison, P., 2002. Quantum Wells, Wires and Dots: Theoretical and Computational Physics. John Wiley & Sons Ltd., New York.

Kittel, C., 1987. Quantum Theory of Solids, second ed. John Wiley & Sons, New York.

Kohlhoff, S., Gumbsch, P., Fischmeister, H.F., 1991. Crack propagation in bcc crystals studied with a combined finite element and atomistic model. Philosophical Magazine A 64, 851–878.

Kunin, I.A., 1982. Elastic Media with Microstructure I, II. Springer-Verlag, New York.

Maradudin, A.A., Montroll, E.W., Weiss, G.H., IPaTova, I.P., 1971. Theory of Lattice Dynamics in the Harmonic Approximation, second ed. Academic Press, New York.

Mura, T., 1987. Micromechanics of Defects in Solids. Martinus Nijhoff, Boston.

Norenberg, H., Briggs, G.A.D., 1999. Si(001) $c(4\times4)$ surface reconstruction: a comprehensive experimental study. Surface Science 430, 154–164.

Pan, E., Yuan, F.G., 2000. Three-dimensional Green's functions in anisotropic bimaterials. International Journal of Solids and Structures 37, 5329–5351.

Rao, S., Hernandez, C., Simmons, J.P., Parthasarathy, T.A., Woodward, C., 1998. Green's function boundary conditions in two-dimensional and three-dimensional atomistic simulations of dislocations. Philosophical Magazine A 77, 231–256.

Shenoy, V.B., Miller, R., Tadmor, E.B., Rodney, D., Phillips, R., Ortiz, M., 1999. An adaptive finite element approach to atomistic-scale mechanics—the quasicontinuum method. Journal of the Mechanics and Physics of Solids 47, 611–642.

Sinclair, J.E., Gehlen, P.C., Hoagland, R.G., Hirth, J.P., 1978. Flexible boundary conditions and nonlinear geometric effects in atomic dislocation modeling. Journal of Applied Physics 49, 3890–3897.

Tadmor, E.B., Ortiz, M., Phillips, R., 1996. Quasicontinuum analysis of defects in solids. Philosophical Magazine A 73, 1529–1563.

Tersoff, J., 1989. Modeling solid-state chemistry: interatomic potentials for multicomponent systems. Physical Review B 39, 5566–5568.

Tewary, V.K., 1973. Green-function method for lattice statics. Advances in Physics 22, 757–810.

Tewary, V.K., 2004. Multiscale Green's-function method for modeling point defects and extended defects in anisotropic solids: Application to a vacancy and free surface in copper. Physical Review B 69, 094109-1-13.

Tewary, V.K., Yang, B., 2003. Multiscale modeling of mechanical response of quantum nanostructures. Materials Research Society Symposium Proceeding 778, U9.2.1.

Ting, T.C.T., 1996. Anisotropic Elasticity. Oxford University Press, Oxford.

Townsend, J.R., 1976. Inhomogeneity corrections to elastic-continuum point-defect models. Physical Review B 14, 5535–5537.

Yang, B., Pan, E., 2003. Elastic fields of quantum dots in multilayered semiconductors: a novel Green's function method. ASME Journal of Applied Mechanics 70, 161–168.